Chemical Research in Toxicology

Article

pubs.acs.org/crt

Comparative Analysis of Four Oxidized Guanine Lesions from Reactions of DNA with Peroxynitrite, Singlet Oxygen, and γ-Radiation

Liang Cui,[†,∥] Wenjie Ye,[†] Erin G. Prestwich,[†] John S. Wishnok,[†,‡] Koli Taghizadeh,[‡] Peter C. Dedon,[†,‡] and Steven R. Tannenbaum*[,†,‡,§]

[†]Department of Biological Engineering, [‡]Center for Environmental Health Sciences, and [§]Department of Chemistry, Massachusetts Institute of Technology, 77 Massachusetts Avenue, Cambridge, Massachusetts 02139, United States

[∥]Singapore-MIT Alliance for Research and Technology, Center for Life Sciences, National University of Singapore, 28 Medical Drive, Singapore 117456

Supporting Information

ABSTRACT: Oxidative damage to DNA has many origins, including irradiation, inflammation, and oxidative stress, but the chemistries are not the same. The most oxidizable base in DNA is 2-deoxyguanosine (dG), and the primary oxidation products are 8-oxodG and 2-amino-imidazolone. The latter rapidly converts to 2,2-diamino-oxazolone (Ox), and 8-oxodG is further oxidized to spiroiminodihydantoin (Sp) and guanidinohydantoin (Gh). In this study, we have examined the dose−response relationship for the formation of the above four products arising in calf thymus DNA exposed to gamma irradiation, photoactivated rose bengal, and two sources of peroxynitrite. In order to carry out these experiments, we developed a chromatographic system and synthesized isotopomeric internal standards to enable accurate and precise analysis based upon selected reaction monitoring mass spectrometry. 8-OxodG was the most abundant products in all cases, but its accumulation was highly dependent on the nature of the oxidizing agent and the subsequent conversion to Sp and Gh. Among the other oxidation products, Ox was the most abundant, and Sp was formed in significantly greater yield than Gh.

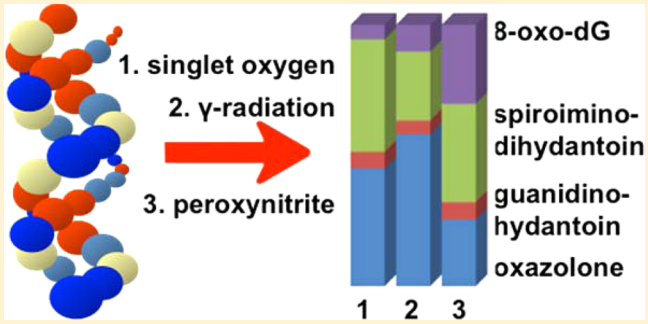

INTRODUCTION

DNA oxidation plays a significant role in the pathophysiology of cancers, aging, and inherited diseases,[1−3] with epidemiological studies demonstrating a strong association between the reactive oxygen (ROS) and nitrogen species (RNS) of chronic inflammation and increased cancer risk.[1−6] This potential for DNA damage to play a causative role in mutation and carcinogenesis has prompted the chemical characterization of oxidatively induced DNA damage and the quest to develop biomarkers that reflect this damage and serve as surrogates for short-lived ROS and RNS.[7] As the most readily oxidized site in DNA, guanine is a major target for DNA oxidants, and its oxidation produces a wide spectrum of end products,[8] including 8-oxo-7,8-dihydro-2′-deoxyguanosine (8-oxodG) spiroiminodihydantoin (Sp) guanidinohydantoin (Gh), 2-amino-5-[2-deoxy-β-D-erythro-pentofuranosyl)amino]-4*H*-imidazol-4-one (imidazolone) and its hydrolysis product, 2,2-diamino-4-[(2-deoxy-β-D-erythro-pentofuranosyl)amino]-5(2*H*)-oxazolone (Ox) (Scheme 1[9]). Although 8-oxodG is produced abundantly in DNA exposed to RNS and ROS,[10−16] it is several orders-of-magnitude more susceptible to further oxidation than dG itself,[17] yielding more stable secondary oxidation products, including Sp and Gh (Scheme 1).[13,18,19] Ox and its precursor imidazolone have been observed as oxidation products of dG or 8-oxodG in oligodeoxynucleotides and calf thymus DNA treated with Mn-TMPyP/$KHSO_5$,[20] peroxynitrite ($ONOO^-$),[19,21] and photochemical oxidants[22−25] (Scheme 1). All of these DNA oxidation products are promutagenic,[10,26−30] with both diastereoisomers of Sp strongly inhibiting DNA polymerase[27,31] and causing mutation frequencies that are at least an order of magnitude higher than those for 8-oxodG.

Therefore, as part of our current focus on inflammation-related DNA damage, including assessment of potential biomarkers, we developed a liquid chromatography-coupled isotope-dilution triple-quadrupole mass spectrometry method (LC-MS/MS) to simultaneously measure 8-oxodG, Sp, Gh, and Ox in DNA and applied the method to DNA treated *in vitro* with $ONOO^-$, singlet oxygen derived from photoactivated rose bengal, and γ-radiation.

Singlet oxygen, with a high quantum yield in aqueous solution, is an important reactive oxygen species *in vivo* and, although accompanied by low levels of other reactive species, is the primary oxidant arising via rose bengal photosensitization.[32,33] γ-Irradiation of aqueous solutions, however, yields hydroxyl radicals and hydrated electrons, with the former causing oxidation of both 2′-deoxyribose and nucleobases in DNA.[34,35] $ONOO^-$ is the product of a reaction of macrophage-

Received: June 30, 2012
Published: November 9, 2012

Scheme 1. Oxidation Products from dG by Various Oxidants

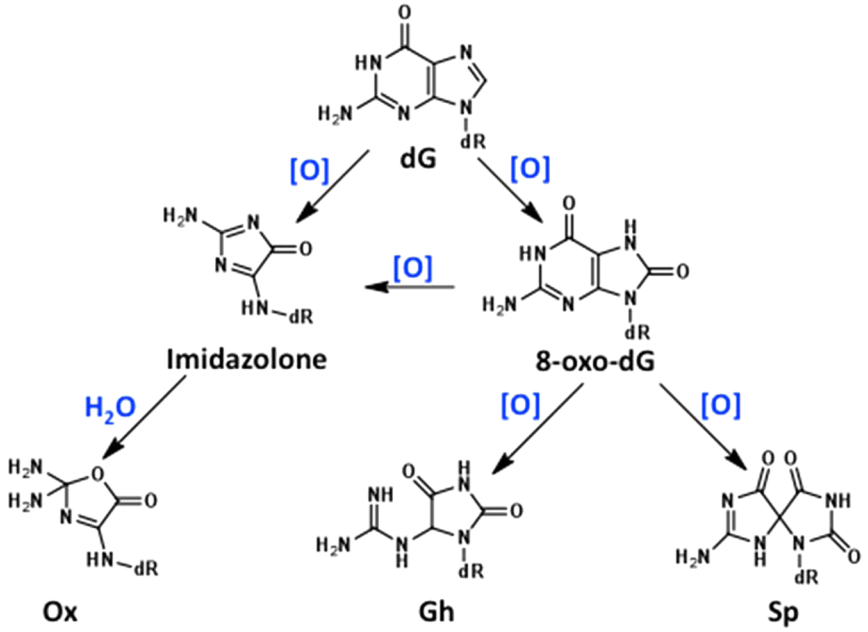

derived nitric oxide and superoxide, and its protonated form undergoes homolytic bond scission to yield a hydroxyl radical and a nitrogen dioxide radical, which are strong and weak oxidants, respectively.[36] The new LC-MS/MS method, which is both more efficient and more sensitive than previous methods, also revealed novel features of the oxidant-specific distribution of these G oxidation products.

EXPERIMENTAL PROCEDURES

Materials and Instruments. Uniformly labeled dG (^{13}C and ^{15}N > 98%) and uniformly labeled ^{15}N dG (≥98%) were obtained from Cambridge Isotope Laboratories (Andover, MA). Benzonase nuclease, deoxyribonuclease (DNase), calf intestine alkaline phosphatase, and calf thymus DNA were from Sigma Aldrich (St. Louis, MO), $ONOO^-$ solution from Cayman Chemical Company (Ann Arbor, MI), phosphodiesterase 1 from USB Products (Cleveland, OH), Nanosep Omega 10 kD exclusion filter columns from Pall Corporation (Ann Arbor, MI), and Sep-Pak C_{18} cartridges from Waters (Milford, Massachusetts). All other chemicals, reagents, and solvents were purchased from Sigma-Aldrich. UV/vis spectroscopy measurements were made on an HP8452 diode-array spectrophotometer (Agilent Technologies, Palo Alto, CA) or a Beckman DU640 diode-array spectrophotometer (Beckman Coulter, Inc., Indianapolis, IN). High-performance liquid chromatography (HPLC) analyses were carried out on an Agilent 1100 Series HPLC system with binary pumps, a degasser, and an autoinjector. Quantitative liquid chromatography–tandem mass spectrometry (LC-MS/MS) analyses were conducted on an Agilent 6430 triple quadrupole mass spectrometer interfaced with an Agilent capillary 1200 binary pumping system or an AB Sciex API 3000 triple quadrupole mass spectrometer (AB Sciex, Framingham, MA) interfaced with an Agilent 1100 binary HPLC. Electrospray ionization mass spectrometry analyses for isotopic purities and structure confirmations by exact mass were done on an Agilent MSD-TOF. Experiments were designed to yield similar levels of Sp across the different oxidation conditions in order to facilitate comparisons. This approach provides a means for comparing relative amounts of the other lesions rather than total amounts of damage.

Synthesis of Standards. ^{15}N-Labeled 8-oxodG was synthesized as described earlier,[37,38] and its identity was confirmed by comparison of its reversed phase HPLC retention time with that of commercially available 8-oxodG, its characteristic UV spectrum (λ_{max}= 248 and 292 nm), and by ESI-MS/MS, which gave a protonated molecular ion with m/z 289 and two fragment ions at m/z 117 and m/z 173, which correspond to the protonated 2′-deoxyribose and $^{15}N_5$-8-oxo-guanine. The standard was quantified by UV spectroscopy using an extinction coefficient of 10,300 M^{-1} cm^{-1} at 293 nm.[39]

The ^{13}C-, ^{15}N-labeled, and unlabeled Sp, Gh, and Ox were synthesized from labeled dG as described previously,[21] and structures were confirmed by UV spectra, HPLC retention times, and ESI-MS/MS. For Sp, ESI-MS/MS analysis yielded a protonated molecular ion at m/z 300.1, along with characteristic fragment ions including m/z 184 and m/z 117.1 (Figure S1b). The molar extinction coefficient for the Sp was determined to be 10,500 M^{-1} cm^{-1} at λ_{max} = 230 nm, which is consistent with the reported value.[21] For Gh, the ESI-MS/MS spectrum (Figure S1c) showed m/z 158.0 as the major fragment released from the protonated Gh (m/z 274.1). For Ox, ESI-MS/MS analysis revealed a protonated molecular ion at m/z 246.7, with fragmentation occurring by both loss of 2-deoxyribose (m/z 131) and loss of CO_2 ($[M + H - CO_2]^+$; m/z 202.9) (Figure S1d). This distinct fragmentation pattern reflects the loss of aromaticity upon oxidation of dG to oxazolone, accompanied by the incorporation of a relatively labile lactone group in the molecule.[9] The major fragment at m/z 87.0 predominated $[BH + H - CO_2]^+$ (Figure S1d).

Reaction of Calf Thymus DNA with Peroxynitrite. Working solutions of $ONOO^-$ were prepared in 0.1 M NaOH by dilution of the commercial stock solution of 100 mM in 0.3 M NaOH, the concentration of which was verified by measuring the absorbance at 302 nm (ε = 1670 M^{-1} cm^{-1}).[40] Aliquots of the working stock solutions of $ONOO^-$ were placed on the side walls of tubes containing a solution of calf thymus DNA (300 μg in 0.4 mL of 25 mM sodium phosphate buffer, pH 7.2) to produce final concentrations of 0–1000 μM. The oxidation reaction was initiated by rapidly vortexing the tube for 1 min and then allowing the reaction to proceed at ambient temperature for 1 h.

Rose Bengal-Mediated Photosensitization. Calf thymus DNA (300 μg, 1 μg/μL in 50 mM sodium phosphate buffer, pH 7.4) was irradiated in the presence or absence of 10 μM rose bengal (added from a dimethyl sulfoxide (DMSO) stock solution) with UV light in a Rayonet RMR-600 reactor with RPR-3500 bulbs (λ_{max} = 350 nm) for 0, 15, 30, 60, or 90 min. The control samples were treated with an equal volume of DMSO and irradiated with UV light for 90 min.

γ-Irradiation. Calf thymus DNA (250 μg, 1 μg/μL) in Chelex-treated 50 mM sodium phosphate buffer at pH 7.4 was exposed to ^{60}Co γ-radiation delivered at 133 Gy/min in a Gammacel-220 (MDS

Nordion, Ottawa, Ontario, Canada), at ambient temperature, for total doses of 0, 7.5, 20, 33, 70, or 133 Gy.

Enzymatic Digestion. Following each of the above treatments, DNA was precipitated by the addition of ethanol to 70%, washed with 70% ethanol, resuspended in 100 μL of water, and quantitated by UV/vis spectroscopy. The DNA was then digested to nucleosides with 4 units of benzonase nuclease, 0.1 units phosphodiesterase 1, 4 units DNase, and 20 units calf intestine alkaline phosphatase in 10 mM Tris buffer (pH 7.9) and 1 mM magnesium chloride. Deferoxamine mesylate (3 mM) and butylated hydroxytoluene (1 mM) were added as antioxidants to inhibit artifactual oxidation. $^{15}N_5$-8-oxodG (1 pmol), $^{13}C_8{}^{15}N_4$-oxazolone (4.25 pmol), $^{13}C_9{}^{15}N_5$-guanidinohydantoin (5 pmol), and $^{13}C_{10}{}^{15}N_5$-spiroiminodihydantoin (2.9 pmol) were added as internal standards and the samples digested for 4 h at 37 °C. Samples were then filtered through 10 kD exclusion filters to remove enzymes and, finally, dried under reduced pressure.

HPLC Prepurification of 2′-Deoxynucleosides to Isolate 8-oxodG, Sp, Gh, and Ox. Digested samples were prepurified using a Varian Microsorb-MV C18 reversed-phase column (5 μm particle, 100 Å pore size, 250 × 4.6 mm) with an acetonitrile/8 mM ammonium acetate gradient. The prepurifications were performed with single 100 μL injections of hydrolyzed DNA samples. Individual fractions were then dried and subjected to LC-MS/MS analysis. The column was maintained at 10 °C with 0.6 mL/min flow rate, and the gradient conditions are detailed in Supporting Information, Table S1. Sp, Gh, and Ox were collected in a single fraction eluting between 3 and 6 min, and 8-oxodG was collected at 14.6−15.6 min (Supporting Information, Table S2). The fractions were dried under reduced pressure.

Quantification of Canonical 2′-Deoxyribonucleosides. To control for DNA losses sustained during DNA workup, canonical 2′-deoxyribonucleosides were quantified by integrating the UV absorbance peaks obtained during HPLC fractionation and summing areas to compare to the 2′-deoxyribonucleoside calibration curves run with each experiment.

LC-MS/MS Analysis of 8-oxodG. The dried samples containing 8-oxodG and the corresponding isotopomer were dissolved in 100 μL of deionized water, and 10 μL were analyzed on an Agilent 6410 tandem quadrupole, or an AB Sciex API 3000, interfaced with an Agilent 1100 series HPLC system. Residual dG was separated from 8-oxodG using isocratic reversed phase chromatography with 200 μL/min, 25 °C, 3% acetonitrile in water with 0.1% acetic acid on a C18 Thermo hypersil gold AQ column (150 × 2, 1 mm, 3 μm particles). It is important to note that 8-oxodG can be formed from dG in-source during ionization; therefore, separation of dG from 8-oxodG is essential for accurate quantitation.[41,42] The mass spectrometers were operated in the positive ion mode, with all instrument parameters optimized for maximum sensitivity. Samples were analyzed in the multiple reaction monitoring mode (MRM), which monitors collision-induced dissociation of a precursor ion to an abundant characteristic product ion. The optimized parameters for the API 3000 were ion source, TurboIonSpray; 200 ms dwell time; declustering potential, 15 V; focusing potential, 90 V; entrance potential, 5 V; collision cell exit potential, 15 V; nebulizer gas, 13 AU (arbitrary unit); curtain gas, 7 AU; collision gas,: 9 AU; temperature, 400 °C; and ion spray voltage, 4,000 V. Samples were analyzed with the following transitions: m/z 284 → 168 for 8-oxodG, m/z 289 → m/z 173 for $^{15}N_5$-labeled 8-oxodG, and m/z 268 → m/z 152 for dG.

LC-MS/MS Analysis of Sp, Gh, and Ox. The fraction containing Sp, Gh, Ox, and their corresponding isotopomers was dried and then redissolved in deionized water (30 μL). ESI-MS/MS analyses were done on an Agilent 6430 triple quadrupole mass spectrometer interfaced with an Agilent capillary 1200 series binary pumping system with a Hypercarb column (100 mm × 1.0 mm, 5 μm particles; Thermo Scientific, Torrance, CA). The gradient was 0.3% formic acid in water (A) and 0.3% formic acid in acetonitrile (B) from 2% to 70% B over 15 min at 20 μL/min (microionization spray capillary). The flow for the first 5 min was diverted to waste. The mass spectrometer was operated in positive ion mode, with instrument parameters optimized for maximal sensitivity (Supporting Information, Table S3). Samples were analyzed in multiple reaction monitoring mode (MRM), using the following transitions: m/z 300 → m/z 184 and m/z 315 → m/z 194 for Sp and uniformly ^{13}C,^{15}N-labeled Sp; m/z 274 → m/z 158 and m/z 288 → m/z 167 for Gh and uniformly ^{13}C,^{15}N-labeled Gh; m/z 247 → m/z 87 and m/z 259 → m/z 93 for Ox and uniformly ^{13}C,^{15}N-labeled Ox, respectively (Figure S1 and Supporting Information, Figure S4).

Preparation of Samples for Calibration Curves. Calibration curves for the labeled and unlabeled forms of each of the four DNA oxidation products were constructed by plotting the MRM signal ratios between the labeled and unlabeled forms against their corresponding concentration ratios. Measurements of 8-oxodG, Sp, Gh, and Ox were based on the MRM signal ratios between analytes of interest and their isotope-labeled internal standards and their respective response curves (Table 1 and Supporting Information, Figure S5).

Table 1. Detection Limits, DNA Requirements, and Parameters for the Preparation of Calibration Curves

lesion	LOD (fmol)[a]	LOQ (fmol)[a]	minimum DNA (μg)	unlabeled standard (fmol)	internal standard (pmol)
8-oxodG	2	5	50	1−10,000	1
Sp	1	3	100	0.2−170	2.9
Gh	1	3	100	0.8−64	5
Ox	3	10	100	10−830	4.25

[a]LOD, limit of detection; LOQ, limit of quantitation.

Determination of LOD/LOQ. The limits of detection (LOD) and quantification (LOQ) of 8-oxodG, Ox, Sp, and Gh were determined by adding known amounts of the corresponding labeled nucleosides to deionized water, followed by LC-MS/MS analysis as described above. The nominal signal-to-noise ratios were ∼3 (LOD) and ∼10 (LOQ). Assuming approximately equal responses for the unlabeled and the labeled nucleosides in the MRM mode, the limit of detection of each oxidation product (the unlabeled nucleoside) was in the range of 1 to 3 fmol, with limits of quantification around 3 to 10 fmol, corresponding to approximately 1−3 nucleoside/10^8 nucleosides in 100 μg of DNA (Table 1)

RESULTS

Method Development. The overall method workflow is outlined in Scheme 2. The first critical step in the method involves artifact-free processing of the oxidized DNA.[7,21] In this case, treated DNA samples were purified by ethanol precipitation, followed by the addition of the antioxidants, deferoxamine mesylate and butylated hydroxytoluene, along with isotopically labeled internal standards. DNA was then enzymatically hydrolyzed with benzonase, phosphodiesterase 1, and deoxyribonuclease (DNase), with dephosphorylation to nucleosides by calf intestine alkaline phosphatase. Following the removal of enzymes by filtration, samples were subjected to HPLC purification of individual 2′-deoxyribonucleosides.

A second critical step in the method involves HPLC prepurification of the various damaged 2′-deoxyribonucleosides. The hydrophilic Sp, Gh, and Ox eluted early on the reversed-phase HPLC system and were collected as a single fraction, while 8-oxodG was well retained on the column. The two groups of 2′-deoxyribonucleosides were collected at the predetermined retention times noted in Experimental Procedures. To quantify the total DNA injected on the HPLC column, canonical 2′-deoxyribonucleosides were quantified by integrating the area under the peaks of the UV absorbance

dx.doi.org/10.1021/tx300294d | Chem. Res. Toxicol. 2013, 26, 195−202

Scheme 2. Experimental Workflow for the Treatment of DNA, Digestion, Sample Preparation, and LC-MS/MS Analysis of 8-oxodG, Sp, Gh, and Ox

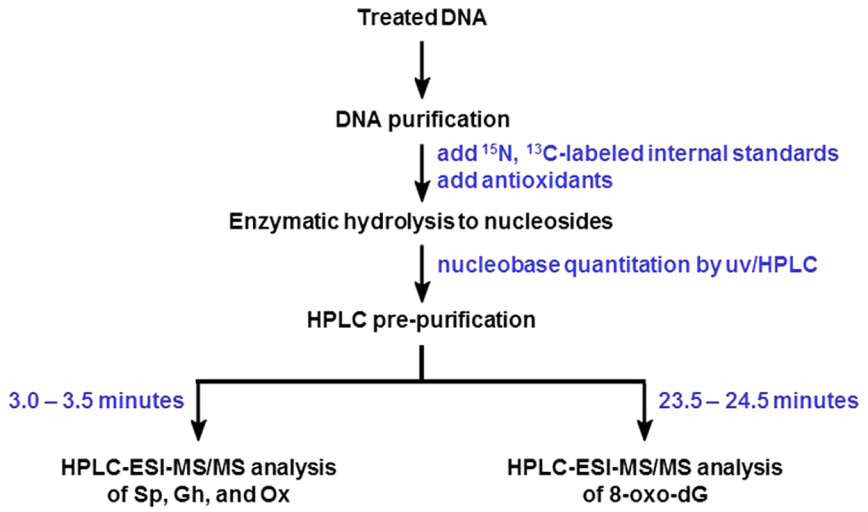

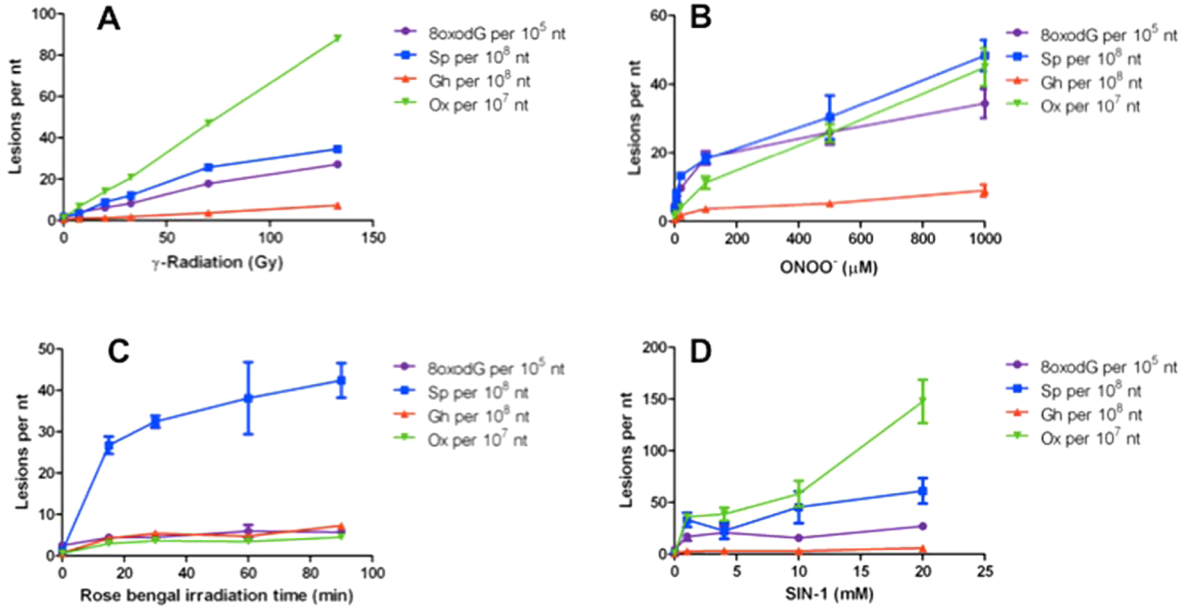

Figure 1. Dose–response curves for G oxidation products with different oxidants. DNA was treated with (a) γ-radiation, (b) $ONOO^-$, (c) $^1O_2$ from photooxidation of rose bengal, and (d) SIN-1, and the G oxidation products 8-oxodG, Sp, Gh, and Ox were quantified as described in Experimental Procedures. Data are plotted as the lesion level without exponential scaling on the *Y*-axis, with the exponential scaling noted in the inset. Data represent the mean ± SD.

profiles obtained during the prepurification steps, with analysis by calibration curves.

The final step of the method involves LC-MS/MS analysis of the individual purified 2′-deoxyribonucleosides. The hydrophilic Sp, Gh, and Ox were optimally resolved on a Hypercarb graphite column using an acetonitrile/water gradient, while 8-oxodG was best resolved using a C18 reversed phase HPLC column, as in the prepurification. Both HPLC systems were coupled to a triple quadrupole mass spectrometer operated in positive ion mode. The Sp and Ox diastereomers were observed with this approach (Supporting Information, Figure S4). Typical detection limits for modified DNA nucleosides were 3–10 fmol (Table 1). For 8-oxodG analysis, the use of a reversed phase column eluted with acetic acid/acetonitrile provided similar MS/MS quantification properties as those reported previously.[7]

Several control studies were performed to assess oxidative artifacts during DNA processing and analysis. The detection and quantitation limits of the guanine oxidation products are listed in Table 1. The dG transition m/z 268 → m/z 152 was monitored to confirm the separation between 8-oxodG and dG and thus to ensure that artifactual production of 8-oxodG in the ion source is not included in the analysis.[41,42] [$^{13}C_{10}$,$^{14}N_5$]-8-oxodG was not detected in the pilot experiments (1 nmol, in triplicate) spiked with [$^{13}C_{10}$,$^{14}N_5$]-dG, which suggests that artifactual formation of 8-oxodG during the sample processing was minimal. To assess the oxidation of 8-oxodG during workup, [$^{15}N_5$]-8-oxodG was added to a DNA sample before enzymatic digestion. Subsequent analysis for [$^{15}N_5$]-Sp, [$^{15}N_5$]-Gh, and [$^{15}N_4$]-Ox was below the detection limits, which demonstrates minimal artifactual formation of Sp, Gh, and Ox during the digestion and workup process.

Analysis of G Oxidation by ONOO⁻, 3-Morpholinosydnonimine (SIN-1), Photoirradiated Rose Bengal, and γ-Radiation. The analytical method was now applied to quantify Sp, Gh, Ox, and 8-oxoG in DNA samples oxidized by four well studied oxidants: ONOO⁻, SIN-1, singlet oxygen arising from photoactivated rose bengal, and γ-radiation. The results are shown in Figures 1 and 2, Table 2, and in Supporting Information Tables S2 and S3. The background levels of damage products in the commercial calf thymus DNA were found to be 2.8 ± 1.4 8-oxodG per 10^5 nt, 4.7 ± 1.9 Sp per 10^8 nt, 0.52 ± 0.11 Gh per 10^8 nt, and 3.6 ± 6.2 Ox per 10^8 nt. The background of 8-oxodG in the calf thymus DNA is higher than the levels observed in cells and tissues[43,44] but is consistent with literature values.[45] As shown in Figure 1, SIN-1 produced nonlinear dose−response curves for all damage products, with ONOO⁻, γ-radiation, and rose bengal photosensitization producing more linear dose−response curves.

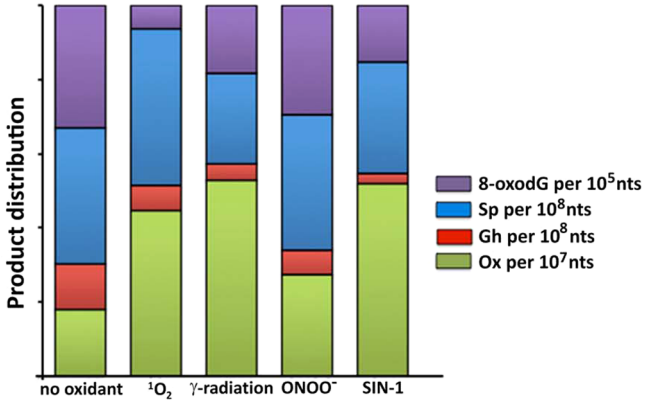

Figure 2. Average amounts of each oxidation product across all measured doses for each oxidant were calculated and presented as a stack plot. The per nucleotide levels chosen were the same as those plotted in Figure 1.

Table 2. Data Summary for DNA Oxidation Products[a]

rose bengal irradiation time (min)	Sp per 10^8 nt	Gh per 10^8 nt	Ox per 10^8 nt	8-oxo per 10^5 nt
0	1.2 ± 0.1	0.7 ± 0.1	6.1 ± 1.7	2.5 ± 0.1
15	27 ± 1.7	4.2 ± 0.4	30 ± 3.7	4.5 ± 0.4
30	33 ± 1.3	5.7 ± 0.7	39 ± 4.5	4.5 ± 0.5
60	38 ± 7.1	4.8 ± 0.4	35 ± 7.3	6 ± 1.3
90	40 ± 3.6	7.6 ± 0.8	43 ± 5.8	5.7 ± 0.7
		γ-Radiation (Gy)		
0	1.7 ± 0.2	0.7 ± 0.1	12 ± 0.08	1.4 ± 0.2
7.5	3.3 ± 0.2	1.0 ± 0.02	138 ± 2.6	3.9 ± 0.1
20	8.9 ± 0.9	1.3 ± 0.1	141 ± 11	6.3 ± 0.2
33	12 ± 1.2	1.9 ± 0.2	207 ± 6.2	8.3 ± 0.4
70	26 ± 1.0	3.7 ± 0.5	470 ± 10	18 ± 0.5
133	35 ± 0.3	7.4 ± 0.3	880 ± 12	27 ± 1.1
		ONOO⁻ (μM)		
0	3.8 ± 0.7	0.7 ± 0.2	14 ± 0.9	4.4 ± 0.5
5	7.3 ± 1.4	1.3 ± 0.4	22 ± 4.9	6.1 ± 1.0
20	13 ± 0.4	1.8 ± 0.02	41 ± 1.5	9.8 ± 0.3
100	18 ± 0.9	3.7 ± 0.04	113 ± 13	18 ± 1.4
500	30 ± 4.5	5.3 ± 0.4	258 ± 18	26 ± 2.5
1000	48 ± 3.7	9 ± 1.4	450 ± 45	34 ± 3.5
		SIN-1 (mM)		
0	1.5 ± 0.1	0.7 ± 0.2	10 ± 3.5	4.4 ± 1.1
1	33 ± 5.7	2.9 ± 0.6	361 ± 32	19 ± 3.4
4	23 ± 6.1	3.2 ± 0.7	388 ± 52	21 ± 5.5
10	46 ± 13	3.0 ± 0.6	585 ± 101	16 ± 0.3
20	61 ± 10	5.9 ± 2.0	1477 ± 172	27 ± 2.4

[a]Data represent the mean ± SD for 3−5 experiments.

DISCUSSION

During chronic inflammation, locally produced ROS and RNS can attack DNA to cause mutation and cell death as part of the pathophysiology of cancer and other diseases.[1−5] As the most readily oxidized of the nucleobases, guanine (G) is preferentially targeted by oxidants and produces a wide spectrum of end products, including 8-oxodG, Sp, Gh, and Ox. 8-OxodG is used widely as a biomarker of G oxidation, whereas other more stable oxidation products, such as Sp, Gh, and Ox, have received relatively little attention in spite of their toxicity and mutagenicity.[46] A previously published method for LC-MS/MS analyses of 8-oxodG, Sp, Gh, and Ox[21] was 10-times less sensitive for Sp and Gh than the present method, with an LOD of about ∼1 lesion per 10^7 nt. Further, the LC-MS/MS method of Sugden and co-workers, which used a reversed-phase HPLC resolution and no prepurification, yielded high background levels of Sp in wild-type *E. coli* cells on the order of 1 Sp per 10^4 to 10^5 nt.[31] In the present studies, we have decreased the detection limits by at least 10-fold to the level of ∼1 lesion per 10^8 nt by employing a prepurification step and appropriate chromatographic systems for resolving the various damage products. In addition, our method gives similar results to those of earlier studies, e.g., for γ-radiation, confirming that our method is accurate.[7,31,35,38,41−45] The more noteworthy result in the analysis of G oxidation products was the strong oxidant dependence of the product spectra. This is illustrated by the dose−response curves in Figure 1 and stacked distribution plots of the average G oxidation products under the different oxidizing conditions shown in Figure 2. Both figures were plotted to permit easy comparisons between oxidizing conditions and relative changes in G oxidation products. Clearly, 8-oxodG is the most abundant product formed with the four oxidants (Figure 1), with Ox consistently observed at higher levels than the other two secondary G oxidation products. These results are consistent with published reports,[9,10,47] in which Ox was found to be the major secondary G oxidation product generated from one- electron oxidants, ONOO⁻, γ-radiation, and singlet oxygen.

Among individual oxidants, the lowest relative levels of 8-oxodG are present with photosensitized $^1O_2$, which correlates with the high relative generation of Sp (Figure 1, Figure 2). Ye et al. reported that Sp was the major secondary oxidation product when guanosine was exposed to rose bengal-photosensitized $^1O_2$ at neutral pH.[48] Our results corroborate the prominence of Sp in $^1O_2$-mediated chemistry, though more Ox was formed in our experiments than in the previous work. This difference is possibly due to the fact that Ye et al. performed their oxidation studies with 2′-deoxynucleosides, whereas we used calf thymus DNA. Previous studies have shown differences in relative ratios of different G oxidation products when using 2′-deoxyribonucleosides and single-stranded and double-stranded oligonucleotides.[49] For γ-radiation, Figure 1A demonstrates linear increases in each G oxidation product examined, with Ox as the predominant product with relatively small proportions of Sp.

dx.doi.org/10.1021/tx300294d | Chem. Res. Toxicol. 2013, 26, 195−202

$ONOO^-$ appears to produce the most even distribution of G oxidation products under the conditions used, as shown in Figure 2. However, Ox remains the most abundant secondary G oxidation product (Table 2) and exists in higher relative proportion as compared to untreated DNA (Figure 2). The high rate of Ox production with $ONOO^-$ is substantiated by the reaction of DNA with SIN-1 that generates $NO^•$ and $O_2^{-•}$ that combine to form $ONOO^-$. The rate of $ONOO^-$ formation from SIN-1 decomposition varies with the medium.[50] In phosphate buffer, the half-life of SIN-1 is estimated to be 14–26 min, with the release of $ONOO^-$ at a rate of 10–12 μM/min.[51−53] Ox is formed in high relative rates (Figure 2) and rapidly increases with higher $ONOO^-$ concentrations. The concentrations of SIN-1 used in this experiment were relatively high compared to those in other studies examining DNA oxidation,[54,55] which is likely the reason that $ONOO^-$ resulted in the highest overall levels of oxidation among the various oxidants (Table 2). Differences in the relative amounts of G oxidation products for $ONOO^-$ and SIN-1 are not surprising given the varying responses observed for the two oxidizing agents by Kim et al.,[55] though that study was looking at more generalized damage. These differing responses are possibly due to other reactive and toxic products formed during the decomposition of SIN-1[56,57] in addition to the effects of sustained lower doses of $ONOO^-$ over time rather than bolus addition. Yu et al.[21] observed a biphasic dose–response curve for 8-oxodG formation by $ONOO^-$ oxidation of DNA, with levels of 8-oxodG increasing up to 2 equivalents of $ONOO^-$, then decreasing until 10 equivalents of $ONOO^-$ were added, and finally increasing again with higher concentrations of $ONOO^-$. Further, they observed that Sp and Gh were formed in DNA in a dose-dependent manner at low $ONOO^-$ concentrations but that the levels of these lesions dropped significantly at high $ONOO^-$ concentrations. In contrast, the lower concentrations of $ONOO^-$ used in the present studies produced a nonlinear but smooth increase in the amounts of 8-oxo-dG, Sp, and Gh in DNA treated with increasing $ONOO^-$ concentrations. The differences could be partially due to the different dosage points monitored, increased number of experimental replicates performed, and higher ratio of dG to $ONOO^-$ in our studies. Yu et al. also observed more artifactual oxidation during digestion and workup as evidenced by the oxidation of labeled dG included in the analysis. When we performed a similar experiment, no oxidation of labeled dG was observed. The $ONOO^-$ used by Yu et al. synthesized via ozonolysis could have different impurities than that purchased for these studies.

In conclusion, a sensitive and specific LC-MS/MS method was developed for the quantification of 8-oxodG, Sp, Gh, and Ox lesions in DNA. Application of the method to DNA oxidized *in vitro* with four different oxidants revealed a clear oxidant dependence of the relative quantities of the G oxidation products.

■ ASSOCIATED CONTENT

Supporting Information

Representative HPLC/UV chromatograms, LC-MS/MS chromatograms, calibration curves, HPLC gradients, elution profiles, LC-MS/MS parameters, standard synthesis schemes, and calculation methods. This material is available free of charge via the Internet at http://pubs.acs.org.

■ AUTHOR INFORMATION

Corresponding Author

*Department of Biological Engineering, 56-731A, Massachusetts Institute of Technology, 77 Massachusetts Avenue, Cambridge, MA 02139. Tel: 617-253-3729. E-mail: srt@mit.edu.

Funding

We acknowledge financial support from the National Cancer Institute (CA26731). Analytical studies were performed in the Bioanalytical Facilities Core of the MIT Center for Environmental Health Sciences, which is supported by a grant from the National Institute of Environmental Health Sciences (ES002109). E.G.P. was supported by an NIEHS Training Grant in Environmental Toxicology 5T32-ES007020-34.

Notes

The authors declare no competing financial interest.

■ ACKNOWLEDGMENTS

We thank Agilent Technologies for graciously providing access to the 6430 triple quadrupole mass spectrometer system.

■ ABBREVIATIONS

LOD, limit of detection; LOQ, limit of quantification; dG, 2-deoxyguanosine; Ox, 2,2-diamino-4-[(2-deoxy-β-D-erythro-pentofuranosyl)amino]-5(2*H*)-oxazolone; Sp, spiroiminodihydantoin; Gh, guanidinohydantoin; ROS, reactive oxygen species; RNS, reactive nitrogen species; Imidazolone, 2-amino-5-[2-deoxy-β-D-erythro-pentofuranosyl)amino]-4*H*-imidazol-4-one; $ONOO^-$, peroxynitrite; LC-MS/MS, liquid chromatography–tandem mass spectrometry; HPLC, high-performance liquid chromatography; ESI, electrospray ionization; DMSO, dimethyl sulfoxide; MRM, reaction monitoring mode; DNase, deoxyribonuclease; SIN-1, 3-morpholinosydnonimine; G, guanine

■ REFERENCES

(1) Coussens, L. M., and Werb, Z. (2002) Inflammation and cancer. *Nature 420*, 860–867.

(2) Klaunig, J. E., and Kamendulis, L. M. (2004) The role of oxidative stress in carcinogenesis. *Annu. Rev. Pharmacol. Toxicol. 44*, 239–267.

(3) Ohshima, H., and Bartsch, H. (1994) Chronic infections and inflammatory processes as cancer risk factors: possible role of nitric oxide in carcinogenesis. *Mutat. Res. 305*, 253–264.

(4) Dedon, P. C., and Tannenbaum, S. R. (2004) Reactive nitrogen species in the chemical biology of inflammation. *Arch. Biochem. Biophys. 423*, 12–22.

(5) Ohshima, H., Tatemichi, M., and Sawa, T. (2003) Chemical basis of inflammation-induced carcinogenesis. *Arch. Biochem. Biophys. 417*, 3–11.

(6) Suerbaum, S., and Michetti, P. (2002) Helicobacter pylori infection. *N. Engl. J. Med. 347*, 1175–1186.

(7) Taghizadeh, K., McFaline, J. L., Pang, B., Sullivan, M., Dong, M., Plummer, E., and Dedon, P. C. (2008) Quantification of DNA damage products resulting from deamination, oxidation and reaction with products of lipid peroxidation by liquid chromatography isotope dilution tandem mass spectrometry. *Nat. Protoc. 3*, 1287–1298.

(8) Henderson, P. T., Neeley, W. L., Delaney, J. C., Gu, F., Niles, J. C., Hah, S. S., Tannenbaum, S. R., and Essigmann, J. M. (2005) Urea lesion formation in DNA as a consequence of 7,8-dihydro-8-oxoguanine oxidation and hydrolysis provides a potent source of point mutations. *Chem. Res. Toxicol. 18*, 12–18.

(9) Matter, B., Malejka-Giganti, D., Csallany, A. S., and Tretyakova, N. (2006) Quantitative analysis of the oxidative DNA lesion, 2,2-

diamino-4-(2-deoxy-beta-D-erythro-pentofuranosyl)amino]-5(2H)-oxazolone (oxazolone), in vitro and in vivo by isotope dilution-capillary HPLC-ESI-MS/MS. *Nucleic Acids Res. 34*, 5449−5460.
(10) Cadet, J., Berger, M., Buchko, G. W., Joshi, P. C., Raoul, S., and Ravanat, J. L. (1994) 2,2-Diamino-4-[(3,5-di-O-acetyl-2-deoxy-beta-D-erythro- pentofuranosyl)amino]-5-(2H)-oxazolone: a novel and predominant radical oxidation product of 3′,5′-di-O-acetyl-2′-deoxyguanosine. *J. Am. Chem. Soc. 116*, 7403−7404.
(11) Luo, W., Muller, J. G., Rachlin, E. M., and Burrows, C. J. (2000) Characterization of spiroiminodihydantoin as a product of one-electron oxidation of 8-Oxo-7,8-dihydroguanosine. *Org. Lett. 2*, 613−616.
(12) Niles, J. C., Burney, S., Singh, S. P., Wishnok, J. S., and Tannenbaum, S. R. (1999) Peroxynitrite reaction products of 3′,5′-di-O-acetyl-8-oxo-7, 8-dihydro-2′-deoxyguanosine. *Proc. Natl. Acad. Sci. U.S.A. 96*, 11729−11734.
(13) Niles, J. C., Wishnok, J. S., and Tannenbaum, S. R. (2001) Spiroiminodihydantoin is the major product of the 8-oxo-7,8-dihydroguanosine reaction with peroxynitrite in the presence of thiols and guanosine photooxidation by methylene blue. *Org. Lett. 3*, 963−966.
(14) Raoul, S., Berger, M., Buchko, G. W., Joshi, P. C., Morin, B., Weinfeld, M., and Cadet, J. (1996) ^{1}H, ^{13}C and ^{15}N nuclear magnetic resonance analysis and chemical features of the two main radical oxidation products of 2-deoxyguanosine: oxazolone and imidazolone nucleosides. *J. Chem. Soc. Perkin. Trans. 2*, 371−381.
(15) Tchou, J., and Grollman, A. P. (1993) Repair of DNA containing the oxidatively-damaged base, 8-oxoguanine. *Mutat. Res. 299*, 277−287.
(16) Yermilov, V., Yoshie, Y., Rubio, J., and Ohshima, H. (1996) Effects of carbon dioxide/bicarbonate on induction of DNA single-strand breaks and formation of 8-nitroguanine, 8-oxoguanine and base-propenal mediated by peroxynitrite. *FEBS Lett. 399*, 67−70.
(17) Uppu, R. M., Cueto, R., Squadrito, G. L., Salgo, M. G., and Pryor, W. A. (1996) Competitive reactions of peroxynitrite with 2′-deoxyguanosine and 7,8-dihydro-8-oxo-2′-deoxyguanosine (8-oxodG): relevance to the formation of 8-oxodG in DNA exposed to peroxynitrite. *Free Radical Biol. Med. 21*, 407−411.
(18) Niles, J. C., Wishnok, J. S., and Tannenbaum, S. R. (2004) Spiroiminodihydantoin and guanidinohydantoin are the dominant products of 8-oxoguanosine oxidation at low fluxes of peroxynitrite: mechanistic studies with ^{18}O. *Chem. Res. Toxicol. 17*, 1510−1519.
(19) Tretyakova, N. Y., Niles, J. C., Burney, S., Wishnok, J. S., and Tannenbaum, S. R. (1999) Peroxynitrite-induced reactions of synthetic oligonucleotides containing 8-oxoguanine. *Chem. Res. Toxicol. 12*, 459−466.
(20) Vialas, C., Claparos, C., Pratviel, G., and Meunier, B. (2000) Guanine oxidation in double-stranded DNA by Mn-TMPyP/$KHSO_5$: 5,8-dihydroxy-7,8-dihydroguanine residue as a key precursor of imidazolone and parabanic acid derivatives. *J. Am. Chem. Soc. 122*, 2157−2167.
(21) Yu, H., Venkatarangan, L., Wishnok, J. S., and Tannenbaum, S. R. (2005) Quantitation of four guanine oxidation products from reaction of DNA with varying doses of peroxynitrite. *Chem. Res. Toxicol. 18*, 1849−1857.
(22) Adam, W., Saha-Moeller, C. R., and Schoenberger, A. (1996) Photooxidation of 8-oxo-7,8-dihydro-2′-deoxyguanosine by thermally generated triplet-excited ketones from 3-(hydroxymethyl)-3,4,4-trimethyl-1,2-dioxetane and comparison with Type I and Type II photosensitizers. *J. Am. Chem. Soc. 118*, 9233−9238.
(23) Adam, W., Andler, S., Saha-Moller, C. R., and Schonberger, A. (1996) Inhibitory effect of ethyl oleate hydroperoxide and alcohol in photosensitized oxidative DNA damage. *J. Photochem. Photobiol. B 34*, 51−58.
(24) Adam, W., Arnold, M. A., Grimm, G. N., Saha-Moller, C. R., Dall'Acqua, F., Miolo, G., and Vedaldi, D. (1998) 4-tert-butylperoxymethyl-9-methoxypsoralen as intercalating photochemical alkoxyl-radical source for oxidative DNA damage. *Photochem. Photobiol. 68*, 511−518.
(25) Adam, W., Grimm, G. N., Saha-Moller, C. R., Dall'Acqua, F., Miolo, G., and Vedaldi, D. (1998) DNA damage by tert-butoxyl radicals generated in the photolysis of a water-soluble, DNA-binding peroxyester acting as a radical source. *Chem. Res. Toxicol. 11*, 1089−1097.
(26) Henderson, P. T., Delaney, J. C., Gu, F., Tannenbaum, S. R., and Essigmann, J. M. (2002) Oxidation of 7,8-dihydro-8-oxoguanine affords lesions that are potent sources of replication errors in vivo. *Biochemistry 41*, 914−921.
(27) Henderson, P. T., Delaney, J. C., Muller, J. G., Neeley, W. L., Tannenbaum, S. R., Burrows, C. J., and Essigmann, J. M. (2003) The hydantoin lesions formed from oxidation of 7,8-dihydro-8-oxoguanine are potent sources of replication errors in vivo. *Biochemistry 42*, 9257−9262.
(28) Klein, J. C., Bleeker, M. J., Lutgerink, J. T., van Dijk, W. J., Brugghe, H. F., van den Elst, H., van der Marel, G. A., van Boom, J. H., Westra, J. G., Berns, A. J., et al. (1990) Use of shuttle vectors to study the molecular processing of defined carcinogen-induced DNA damage: mutagenicity of single O4-ethylthymine adducts in HeLa cells. *Nucleic Acids Res. 18*, 4131−4137.
(29) Moriya, M., Ou, C., Bodepudi, V., Johnson, F., Takeshita, M., and Grollman, A. P. (1991) Site-specific mutagenesis using a gapped duplex vector: a study of translesion synthesis past 8-oxodeoxyguanosine in *E. coli*. *Mutat. Res. 254*, 281−288.
(30) Wood, M. L., Dizdaroglu, M., Gajewski, E., and Essigmann, J. M. (1990) Mechanistic studies of ionizing radiation and oxidative mutagenesis: genetic effects of a single 8-hydroxyguanine (7-hydro-8-oxoguanine) residue inserted at a unique site in a viral genome. *Biochemistry 29*, 7024−7032.
(31) Hailer, M. K., Slade, P. G., Martin, B. D., and Sugden, K. D. (2005) Nei deficient *Escherichia coli* are sensitive to chromate and accumulate the oxidized guanine lesion spiroiminodihydantoin. *Chem. Res. Toxicol. 18*, 1378−1383.
(32) Valenzeno, D. P. (1987) Photomodification of biological membranes with emphasis on singlet oxygen mechanisms. *Photochem. Photobiol. 46*, 147−160.
(33) Gottschalk, P., Paczkowski, J., and Neckers, D. C. (1986) Factors influencing the quantum yields for rose bengal formation of singlet oxygen. *J. Photochem. 35*, 277−281.
(34) Buxton, G. V., Greenstock, C. L., Helman., W. P., and Ross, A. B. (1988) Critical review of rate constants for eations of hydrated electrons, hydrogen atoms and hydroxyl radicals ($\cdot OH/\cdot O^-$) in acqueous solution. *J. Phys. Chem. Ref. Data 17*, 513−886.
(35) Ward, J. F. (1988) DNA damage produced by ionizing radiation in mammalian cells: identities, mechanisms of formation, and reparability. *Prog. Nucleic Acid Res. Mol. Biol. 35*, 95−125.
(36) Szabo, C., Ischiropoulos, H., and Radi, R. (2007) Peroxynitrite: biochemistry, pathophysiology and development of therapeutics. *Nat. Rev. Drug Discovery 6*, 662−680.
(37) Brodie, B. B., Axelrod, J., Shore, P. A., and Udenfriend, S. (1954) Ascorbic acid in aromatic hydroxylation. II. Products formed by reaction of substrates with ascorbic acid, ferrous ion, and oxygen. *J. Biol. Chem. 208*, 741−750.
(38) Singh, R., McEwan, M., Lamb, J. H., Santella, R. M., and Farmer, P. B. (2003) An improved liquid chromatography/tandem mass spectrometry method for the determination of 8-oxo-7,8-dihydro-2′-deoxyguanosine in DNA samples using immunoaffinity column purification. *Rapid Commun. Mass Spectrom. 17*, 126−134.
(39) Kasai, H., and Nishimura, S. (1984) Hydroxylation of deoxyguanosine at the C-8 position by ascorbic acid and other reducing agents. *Nucleic Acids Res. 12*, 2137−2145.
(40) Hughes, M. N., and Nicklin, H. G. (1968) The chemistry of pernitrites. Part I. Kinetics of decomposition of pernitrous acid. *J. Chem. Soc., A 0*, 450−452.
(41) Dizdaroglu, M., Jaruga, P., and Rodriguez, H. (2001) Measurement of 8-hydroxy-2′-deoxyguanosine in DNA by high-performance liquid chromatography-mass spectrometry: comparison with measurement by gas chromatography-mass spectrometry. *Nucleic Acids Res. 29*, E12.

(42) Ravanat, J. L., Duretz, B., Guiller, A., Douki, T., and Cadet, J. (1998) Isotope dilution high-performance liquid chromatography-electrospray tandem mass spectrometry assay for the measurement of 8-oxo-7,8-dihydro-2′-deoxyguanosine in biological samples. *J. Chromatogr., B 715*, 349−356.
(43) Hamilton, M. L., Guo, Z., Fuller, C. D., Van Remmen, H., Ward, W. F., Austad, S. N., Troyer, D. A., Thompson, I., and Richardson, A. (2001) A reliable assessment of 8-oxo-2-deoxyguanosine levels in nuclear and mitochondrial DNA using the sodium iodide method to isolate DNA. *Nucleic Acids Res. 29*, 2117−2126.
(44) Mangal, D., Vudathala, D., Park, J. H., Lee, S. H., Penning, T. M., and Blair, I. A. (2009) Analysis of 7,8-dihydro-8-oxo-2′-deoxyguanosine in cellular DNA during oxidative stress. *Chem. Res. Toxicol. 22*, 788−797.
(45) Ravanat, J. L., Douki, T., Duez, P., Gremaud, E., Herbert, K., Hofer, T., Lasserre, L., Saint-Pierre, C., Favier, A., and Cadet, J. (2002) Cellular background level of 8-oxo-7,8-dihydro-2′-deoxyguanosine: an isotope based method to evaluate artefactual oxidation of DNA during its extraction and subsequent work-up. *Carcinogenesis 23*, 1911−1918.
(46) Kaur, H., and Halliwell, B. (1994) Evidence for nitric oxide-mediated oxidative damage in chronic inflammation. Nitrotyrosine in serum and synovial fluid from rheumatoid patients. *FEBS Lett. 350*, 9−12.
(47) Ravanat, J. L., and Cadet, J. (1995) Reaction of singlet oxygen with 2′-deoxyguanosine and DNA. Isolation and characterization of the main oxidation products. *Chem. Res. Toxicol. 8*, 379−388.
(48) Ye, Y., Muller, J. G., Luo, W., Mayne, C. L., Shallop, A. J., Jones, R. A., and Burrows, C. J. (2003) Formation of ^{13}C-, ^{15}N-, and ^{18}O-labeled guanidinohydantoin from guanosine oxidation with singlet oxygen. Implications for structure and mechanism. *J. Am. Chem. Soc. 125*, 13926−13927.
(49) Fleming, A. M., Muller, J. G., Ji, I., and Burrows, C. J. (2011) Characterization of 2′-deoxyguanosine oxidation products observed in the Fenton-like system Cu(II)/H_2O_2/reductant in nucleoside and oligodeoxynucleotide contexts. *Org. Biomol. Chem. 9*, 3338−3348.
(50) Martin-Romero, F. J., Gutierrez-Martin, Y., Henao, F., and Gutierrez-Merino, C. (2004) Fluorescence measurements of steady state peroxynitrite production upon SIN-1 decomposition: NADH versus dihydrodichlorofluorescein and dihydrorhodamine 123. *J. Fluoresc. 14*, 17−23.
(51) Brunelli, L., Crow, J. P., and Beckman, J. S. (1995) The comparative toxicity of nitric oxide and peroxynitrite to Escherichia coli. *Arch. Biochem. Biophys. 316*, 327−334.
(52) Cuddy, L. K., Gordon, A. C., Black, S. A., Jaworski, E., Ferguson, S. S., and Rylett, R. J. (2012) Peroxynitrite donor SIN-1 alters high-affinity choline transporter activity by modifying its intracellular trafficking. *J. Neurosci. 32*, 5573−5584.
(53) Doulias, P. T., Barbouti, A., Galaris, D., and Ischiropoulos, H. (2001) SIN-1-induced DNA damage in isolated human peripheral blood lymphocytes as assessed by single cell gel electrophoresis (comet assay). *Free Radical Biol. Med. 30*, 679−685.
(54) Delaney, S., Delaney, J. C., and Essigmann, J. M. (2007) Chemical-biological fingerprinting: probing the properties of DNA lesions formed by peroxynitrite. *Chem. Res. Toxicol. 20*, 1718−1729.
(55) Kim, M. Y., Dong, M., Dedon, P. C., and Wogan, G. N. (2005) Effects of peroxynitrite dose and dose rate on DNA damage and mutation in the supF shuttle vector. *Chem. Res. Toxicol. 18*, 76−86.
(56) Bohn, H., and Schonafinger, K. (1989) Oxygen and oxidation promote the release of nitric oxide from sydnonimines. *J. Cardiovasc. Pharmacol. 14*, S6−12.
(57) Konishi, K., Watanabe, N., and Arai, T. (2009) SIN-1 cytotoxicity to PC12 cells is mediated by thiol-sensitive short-lived substances generated through SIN-1 decomposition in culture medium. *Nitric Oxide 20*, 270−278.